Enhancement of luminescence intensity and increase of emission lifetime in Eu^{3+}-doped $3CdO–Al_2O_3–3SiO_2$ amorphous system

Yan Cong[a,b], Bin Li[a,*], Bingfu Lei[a,b], Xiaojun Wang[a], Chunxu Liu[a], Junye Liu[a], Wenlian Li[a]

[a]*Key Laboratory of Excited State Processes, Changchun Institute of Optics, Fine Mechanics and Physics, Chinese Academy of Sciences, Changchun 130033, PR China*
[b]*Graduate School of the Chinese Academy of Sciences, Chinese Academy of Sciences, Beijing 100039, PR China*

Abstract

Intense photoluminescence at room temperature was observed in amorphous cadmium aluminum silicate doped with europium prepared by the sol–gel method. The structure of the $3CdO–Al_2O_3–3SiO_2{:}Eu^{3+}$ system ($CAS{:}Eu^{3+}$) has been determined by transmission electron microscopy (TEM) and X-ray diffraction (XRD). The excitation and the emission spectra indicated that the red characteristic emission (611 nm) of $CAS{:}Eu^{3+}$ under UV excitation due to $^5D_0 \rightarrow {}^7F_2$ electric dipole transition is the strongest. Both XRD data and the emission ratio of $(^5D_0 \rightarrow {}^7F_2)/(^5D_0 \rightarrow {}^7F_1)$ reveal that the Eu^{3+} is in a site without inversion symmetry. The maximum photoluminescence intensity has been obtained for 25 mol% concentration of Eu^{3+} in CAS, and the intensity enhancement and lifetime increase of Eu^{3+} with increasing sintering temperature were observed due to the less OH-content in the samples.
© 2007 Elsevier B.V. All rights reserved.

Keywords: Intensity increasing and lifetime lengthening; Sol–gel; Europium; OH-content

1. Introduction

Both the amorphous and crystalline metal silicates are of interest for their useful physical and chemical properties. Recently, much attention has been devoted to the behavior of amorphous silica glasses which are widely used in optical areas [1]. Compared with polycrystals, glasses have many advantageous applications, such as easy-made, scale-varied, easy to be optic fiber and adjustable host composition. For example, amorphous cadmium aluminum silicate glasses have been intensely investigated due to their development in fiber telecommunications and other areas [2]. Compared with the other methods, the sol–gel process is more suitable for the deposition of amorphous glasses because of the advantages of this "wet-chemistry": possible fabrication of porous as well as dense silica samples, a low temperature process as compared to the conventional melting procedures (up to 2000 °C), and

feasibility of homogenous doping with metal ions. All of these advantages have led to the method to make materials with specific optical and electrical properties [3]. The amorphous sol–gel glasses have been reported as promising host materials for highly doped with transition metal ions and rare-earth ions [4,5]. Many trivalent rare-earth ions such as Eu^{3+}, Tm^{3+}, Er^{3+} and Pr^{3+} were used to dope as absorption and emission centers in these materials [6,7]. Among the rare-earth ions, Eu^{3+} is the most popular as one of the most efficient ions. Eu^{3+} ion-doped sol–gel glasses show thermal broadening of the spectral lines and change in the excitation spectra in the gel-to-glass conversion [8]. The Eu^{3+} ions present good luminescence performance in different bulk host materials and films [9–12], and also are particularly suitable for applications as activators due to their well-defined transitions within the 4f shell [13].

In this work, a new amorphous material, Eu^{3+}-doped $3CdO–Al_2O_3–3SiO_2$ system with different dopant contents, was prepared by the sol–gel method and its luminescence properties were investigated. The enhancement of

*Corresponding author. Tel./fax: +86 431 86176935.
E-mail address:* lib020@ciomp.ac.cn (B. Li).

luminescence intensity and the increase of Eu^{3+} emission lifetime with increasing of sintering temperature were observed. The results were attributed to the less OH-content in the samples.

2. Experiment

2.1. Preparation

The $Cd_{3-x}Eu_xAl_2Si_3O_{12}$ samples, with $x = 10$–40 mol%, were prepared by sol–gel method. The starting materials with the 99.99% purity were cadmium nitrate ($Cd(NO_3)_2 \cdot 4H_2O$), aluminum nitrate ($Al(NO_3)_3 \cdot 9H_2O$), tetraetoxysilane (TEOS) and europium nitrate ($Eu(NO_3)_3 \cdot 6H_2O$). TEOS was dissolved in the ethanol under vigorous stirring. Hydrolysis took place upon addition of distilled water and the final molar ratio of TEOS:ethanol:water was 1:12:4. About half an hour later, $Al(NO_3)_3$, $Cd(NO_3)_2$ and $Eu(NO_3)_3$ were added to it. Stirring the solution homogeneously and keeping the pH at 2–3, then the solution was kept at $60\,^\circ C$ till gel was formed. The gel was dried at $80\,^\circ C$ and the powder was obtained. The powder was sintered at 500, 600, 700, and $800\,^\circ C$ for 3 h, respectively, to get the desired phase. When the temperature was increased to $900\,^\circ C$, the sample melted.

2.2. Characterization

The X-ray diffraction (XRD) data were collected by a Rigaku D/max-IIB X-ray powder diffractometer using Cu Kα1 ($\lambda = 0.15,405$ nm) radiation. A DT-30 Shimadzu thermal analyzer was used for recording thermogravimetric and differential thermal analysis (TG-DTA) curves for the CAS:Eu^{3+} gel powders. The excitation and emission spectra were performed on a Hitachi F-4500 fluorescence spectrophotometer equipped with a 150 W Xenon lamp as the excitation source. Fluorescence decay curves of Eu^{3+} were measured using a modulated light source and a computer controlled digitizing oscilloscope.

3. Results and discussion

The TG-DTA curves of the sample are shown in Fig. 1. The first clear weight loss at RT-$200\,^\circ C$, possibly corresponds to dehydration of adsorbed H_2O and also Si–OH and Al–OH originated from adsorbing ethanol when the gel was prepared. The second weight loss below $600\,^\circ C$, with two exothermic peaks, belongs to the evaporation and combustion of organic chemicals. Above $600\,^\circ C$, no clear weight loss and endo- or exothermal feature can be observed in Fig. 1. There is another weight loss at about $850\,^\circ C$; this perhaps results from the decomposition of CdO.

The XRD patterns of the samples show the absence of crystalline. The broad peak is due to the amorphous structure of the samples, and the addition of Eu^{3+} does not alter the amorphous nature of the powders. The least
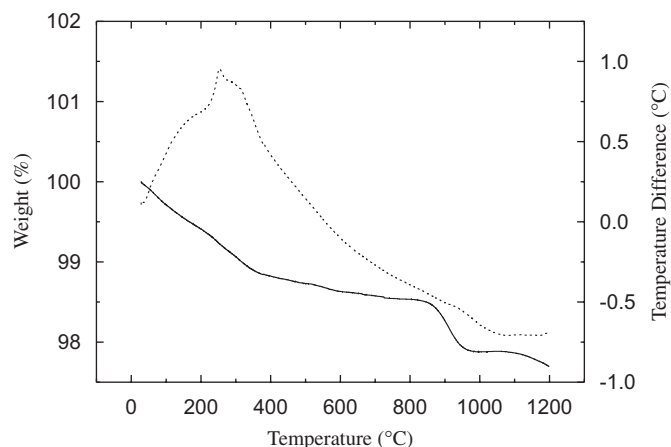

Fig. 1. TG curve (solid line) and DTA curve (dotted line) of $3CdO$–Al_2O_3–$3SiO_2$ doped with Eu^{3+} ion obtained at $800\,^\circ C$ for 3 h.

particle size in the $800\,^\circ C$ sintered sample is about $0.5\,\mu m$ as demonstrated by transmission electron microscopy (TEM), and the pattern gives no evidence of any periodic structure, confirming the amorphous character.

The excitation spectrum (Fig. 2) monitored at 611 nm (Eu^{3+} emission) exhibits the excitation sharp lines, assigned respectively to the transitions between the ground level $^7F_0$ and the excited levels ^5H_J, $^5D_4$, ^5G_J, $^5L_6$, $^5D_{3,2,1}$. The strongest one peaks at 394 nm, which consists of unresolved bands due to the f–f multiplets of the Eu^{3+} excited state. The spectrum also depicts a broad band centered at 270 nm, corresponding to the ligand-to-Eu^{3+} charge-transfer transitions (LMCT) [14] overlapped with the $^7F_0 \rightarrow {}^5H_J$ transition.

The emission intensity of CAS doped with 25 mol% Eu^{3+} is measured under excitation $\lambda_{ex} = 394$ nm as shown in Fig. 3a. The spectrum consists of profiles mainly located in the red spectral area (from 575 to 630 nm), corresponding to transitions from the excited $^5D_0$ state to ^7F_J ($J = 0$, 1, 2, 3, 4) levels of $4f^6$ configuration of Eu^{3+} [15]. The dominant emission peak situated at 611 nm is due to the $^5D_0 \rightarrow {}^7F_2$ electric dipole transition.

Upon excitation of 254 nm, there exists a broad band emission with the maximum located at 400 nm, as shown in Fig. 3b, in addition to the four peaks discussed above in the emission spectrum of Eu^{3+}-doped CAS phosphor. The broad band can be assigned to the emission from localized electron–hole pairs, self-trapped excitons (STE), and this broad feature also exists in the Eu^{3+} free samples [16].

To the best of our knowledge, the $^5D_0 \rightarrow {}^7F_1$ magnetic dipole transition insensitive to the site symmetry is dominating, when the Eu^{3+} ions embedded in a site with inversion symmetry, while in a site without inversion symmetry the $^5D_0 \rightarrow {}^7F_2$ electric dipole transition, induced by the lack of inversion symmetry at the Eu^{3+} site, is the strongest [15,17,18]. As shown in Fig. 3, the $^5D_0 \rightarrow {}^7F_2$ at 611 nm is stronger than the transition to the $^7F_1$ state at
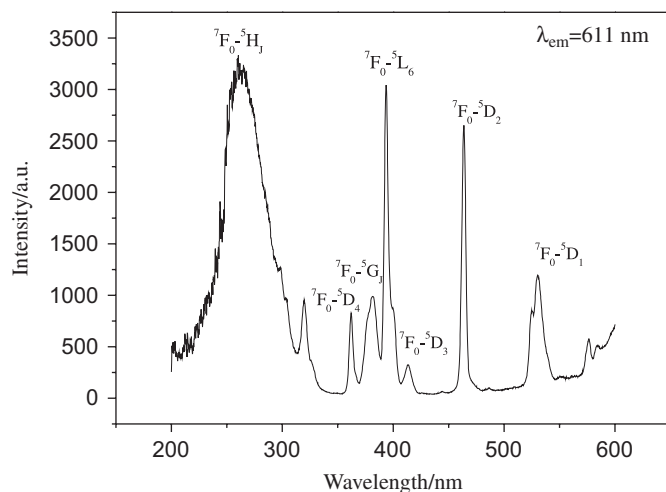
Fig. 2. Excitation ($\lambda_{em} = 611$ nm) spectrum of 3CdO–Al$_2$O$_3$–3SiO$_2$:Eu^{3+} (25% molar ratio) calcined at 800 °C.
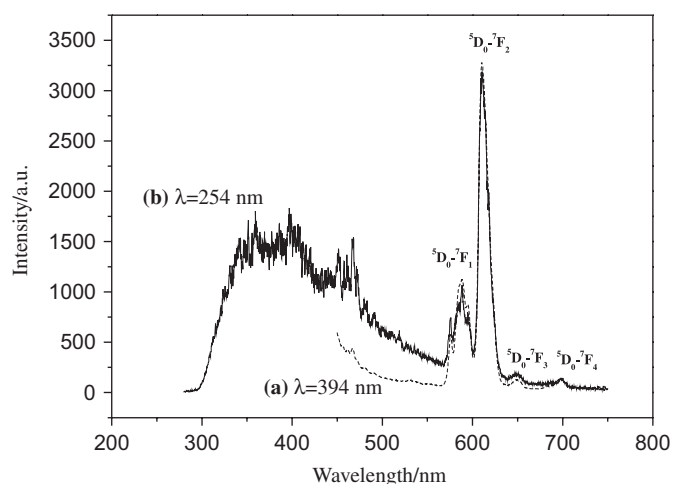
Fig. 3. Emission spectra of 3CdO–Al$_2$O$_3$–3SiO$_2$:Eu^{3+} (25% molar ratio) sintered at 800 °C: (a) excitation of 394 nm and (b) excitation of 254 nm.

Fig. 4. Dependence of the emission intensity of Eu^{3+} with its doping concentration.

588 nm. So as in agreement with the XRD results, the addition of Eu^{3+} ion does not alter the amorphous nature of the powders. Eu^{3+} ion is in a site without inversion symmetry. As seen from the emission spectrum (Fig. 3), the emissions from $^5D_2$ and $^5D_1$ are quenched because the higher energy level emission can be quenched in favor of the lower energy level emission. If the Eu^{3+} concentration is high enough, the following cross-relaxations may occur [19]:
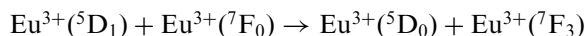
$$Eu^{3+}(^5D_1) + Eu^{3+}(^7F_0) \rightarrow Eu^{3+}(^5D_0) + Eu^{3+}(^7F_3)$$

Fig. 4 shows the dependence of the relative emission intensity of Eu^{3+} ($^5D_0 \rightarrow {}^7F_2$ transition at 611 nm) with its molar concentration in the samples sintered at 800 °C. The Eu^{3+} emission intensity initially increases as the doping concentration increases, reaching a maximum at 25 mol%. The intensity then decreases for higher Eu^{3+} concentrations due to the concentration quenching effect.
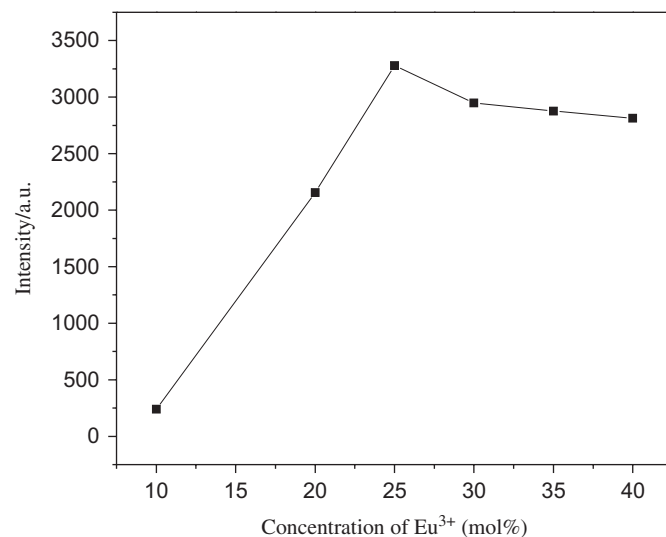
3.1. The emission spectra of CAS

Twenty-five percent Eu^{3+} after sintering at different temperatures from 500 to 800 °C are presented in Fig. 5. It is known from the figure that the Eu^{3+} emission intensity increases with increasing the heat treatment temperature. The enhancement of the intensity is partially explained by the increase of dehydration of the host. In fact, OH$^-$ ions are easily introduced into the host matrix due to the nature of the wet-chemical route. As the as-synthesized sample is heated to a higher temperature, a large number of OH-groups can be removed. OH$^-$ vibration frequencies occurring in the broad range of 2700–3700 cm^{-1} is much higher than other vibrations [20]. As a result, only a few phonons are required for non-radiative de-excitation of $^5D_0$ state. OH$^-$ ions are thus believed to be very efficient quenchers of the luminescence of Eu^{3+} through multiphonon relaxation.

The effect of sintering temperature on the photoluminescence decay curves of the CAS:Eu^{3+} $^5D_0 \rightarrow {}^7F_2$ red emission is also investigated. As shown in Fig. 6, the decay curves can be fitted by the exponential function $I = A_1\exp(-t/\tau_1) + A_2\exp(-t/\tau_2)$, where τ_1 and τ_2 are, respectively, the short- and long-decay components, and the results are shown in Table 1. It is well known that the sol–gel derived materials are usually micro-heterogeneous because the different sites environment. Thus, the Eu^{3+} in different sites possess varies excited state lifetime values due to their different micro-environment. The average lifetime $<\tau>$ is given by $<\tau> \geqslant (A_1\tau_1^2 + A_2\tau_2^2)/(A_1\tau_1 + A_2\tau_2)$. The lifetime of Eu^{3+} increases with increasing heat treatment temperature for the samples, resulting from the reduction of OH groups on heating. The fluorescence lifetime of Eu^{3+} is sensitive to the OH oscillators. As in agreement with the effect of sintering temperature on emission intensity results (the emission
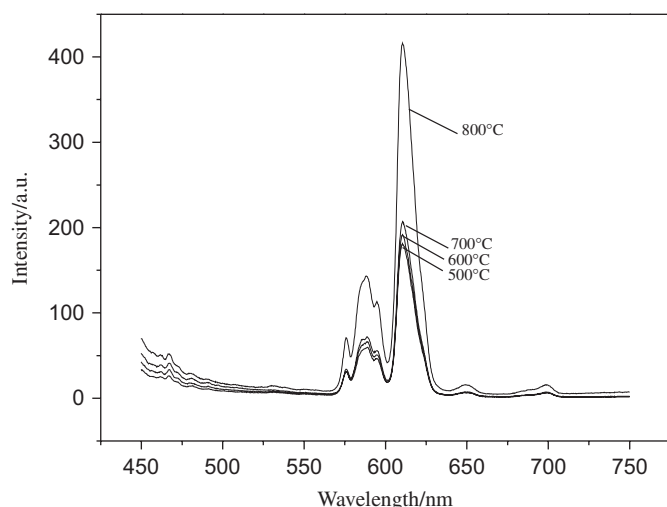
Fig. 5. Effect of heating temperature on emission ($\lambda_{ex} = 394$ nm) spectra of $3CdO-Al_2O_3-3SiO_2$:25 mol% Eu^{3+}.

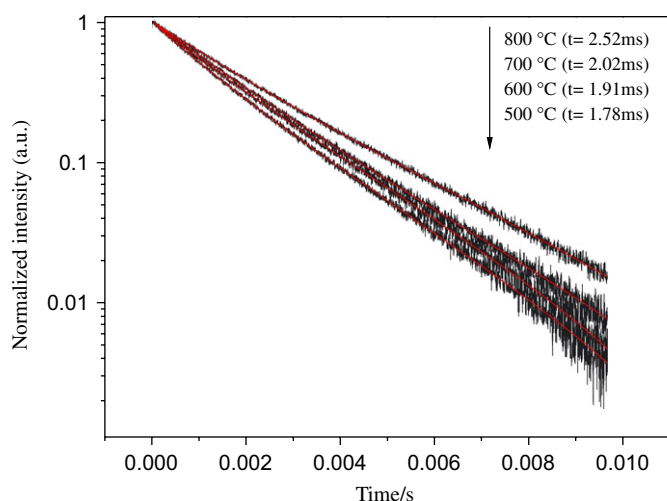Fig. 6. Photoluminescence decay curves of the Eu^{3+} $^5D_0 \rightarrow {}^7F_2$ red emission excited at 266 nm for the 25 mol% Eu^{3+} samples at different sintering temperatures.

Table 1
Decay times of the CAS:Eu^{3+} sintered in different temperatures

Sample (T_{anneal}, °C)	Decay lifetimes (ms)		
	T_1	T_2	T
a (800)	1.5	2.83	2.52
b (700)	1.38	2.37	2.02
c (600)	2.04	0.95	1.91
d (500)	1.96	0.90	1.78

intensity of the sample sintered at 800 °C is much greater than that of other samples), the lifetimes show no apparent increase in the samples when sintered from 500 to 700 °C. The lifetime of sample calcined at 800 °C, however, is much longer than that of the other three samples, indicating that the elimination of OH groups nearly completes at 800 °C. The decrease of the impurities results in the increase of the

Fig. 7. FTIR spectra of the 25 mol% Eu^{3+}-doped samples at different sintering temperatures.

lifetime of Eu^{3+}. The effects of heating on water contamination in the samples were also studied by the IR spectroscopy as shown in Fig. 7. The peaks at about 1700 and a broad band ranging from 3000 to 3700 cm^{-1} are characteristic of the vibration of OH groups. The intensity of the OH band associated with H_2O molecules decreased with the increasing of the heat temperature markedly.

4. Conclusion

In conclusion, Eu^{3+}-doped CAS was synthesized used the sol–gel method. Bright red luminescence at 611 nm attributed to $^5D_0 \rightarrow {}^7F_2$ transition was observed upon 394 nm excitation. The maximum PL intensity of CAS with the Eu^{3+} concentration of 25 mol% was achieved, after that quenching occurs. The removing of a number of OH groups may well explain both the enhancement of luminescence intensity and the increase of lifetime in the Eu^{3+}-doped CAS system. The origin of the substantial increase of luminescent intensity is the significant decrease of OH$^-$ ions. Therefore, effectively eliminating OH-groups will greatly improve the luminescent efficiency.

Acknowledgments

References

[1] C.J. Brinker, G.W. Scherer, Sol–Gel Science, Academic Press, New York, 1990.
[2] L.H. Huang, X.R. Liu, H. Lin, J.L. Lin, Appl. Phys. Lett. 77 (2000) 2849.
[3] C.K. Joergensen, R. Reisfeld, Struct. Bond. 50 (1982) 121.

[4] M. Morita, N. Miyazaki, M. Herren, D. Rau, J. Lumin. 76–77 (1998) 238.

[5] D.E. Harrison, V. Hoffman, J. Electrochem. Soc. 106 (1959) 800.

[6] H. Higuchi, M. Takahashi, Y. Kawamoto, K. Kadono, T. Ohtsuki, N. Peyghambarian, N. Kitamura, J. Appl. Phys. 83 (1998) 19.

[7] M. Tsuda, K. Soga, H. Inoue, S. Inoue, A. Makishima, J. Appl. Phys. 85 (1999) 29.

[8] X. Fan, M. Wang, G. Xiong, Mater. Sci. Eng. B 21 (1993) 55.

[9] A.M. Srivastava, J. Lumin. 69 (1996) 301.

[10] M. Dejneka, E. Snitzer, R.E. Riman, Y. Gao, C.S. Shi, J. Phys. Chem. Solids 57 (1996) 1303.

[11] R. Ternane, M. Trabelsi-Ayedi, N. Kbir-Ariguib, B. Piriou, J. Lumin. 81 (1999) 165.

[12] R. Reisfeld, M. Zelner, A. Patra, J. Alloys Compd. 300–301 (2000) 147.

[13] G. Blasse, Handbook on the Physics and Chemistry of Rare Earths, vol. 4, North Holland, Amsterdam, 1979, p. 237.

[14] Y.C. Chen, Y.H. Chang, B.S. Tsai, Opt. Mater. 27 (2005) 1847.

[15] G. Blasse, B.C. Geiabmaier, Luminescent Materials, Springer, Berlin, 1994, p. 117.

[16] B. Lei, Y. Liu, Z. Ye, C. Shi, Chem. Lett. 32 (2003) 904.

[17] B.R. Judd, Phys. Rev. 127 (1962) 511.

[18] G.S. Ofelt, J. Chem. Phys. 37 (1962) 511.

[19] A.H. Kitai, Solid State Luminescence, Chapman & Hall, London, 1993, p. 38.

[20] L. Zhang, F. Hu, J. Phys. Chem. Solids 63 (2002) 575.